New J. Chem., 1991, **15**, 417-430

MONODENTATE CARBOXYLATE COMPLEXES AND THE CARBOXYLATE SHIFT: IMPLICATIONS FOR POLYMETALLOPROTEIN STRUCTURE AND FUNCTION

R. Lynn Rardin, William B. Tolman and Stephen J. Lippard *

Department of Chemistry, Massachusetts Institute of Technology, Cambridge, Massachusetts 02139 U.S.A.

Received August 20, accepted December 17, 1990.

ABSTRACT. — Carboxylates serve as an important class of ligands in inorganic chemistry and biology. Of the various types of metal-carboxylate binding modes, monodentate bridging between metal centers offers unique flexibility. More than 30 complexes containing this structural motif have been characterized, many of them recently. Through a detailed analysis of their stereochemistry, it has been possible to arrange these complexes into three classes, depending upon the strength of the interaction of the "dangling" oxygen atom of the carboxylate group with one of the bridged metal atoms. The monodentate bridging mode is postulated to be an important intermediate between the other, more common, carboxylate attachment modes, based on observed variations of the geometry for monodentate bridges in structurally characterized complexes. The movement from monodentate bridging to these other binding modes, termed the "carboxylate shift", is analyzed for the three classes of carboxylate bridged complexes. Such a shift could be kinetically important in carboxylate containing metalloproteins.

Introduction

Simple carboxylate anions are ubiquitous and versatile ligands in coordination chemistry. [1-4] Numerous complexes with a variety of elements have been prepared, many of which have played key roles in the conceptual development of modern inorganic chemistry. Perhaps most striking in terms of their impact are the so called dinuclear "paddlewheel" and trinuclear "basic" carboxylate complexes (Figure 1).

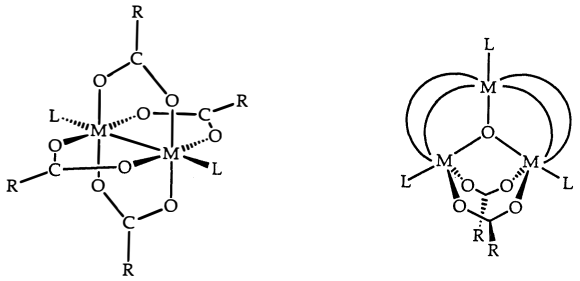

Figure 1. – Paddlewheel (left) and trinuclear basic carboxylate (right) complexes. Curved lines represent bridging carboxylate groups.

Extensive structural and physicochemical studies of these species have been crucial for increasing our understanding of bonding and magnetic interactions between proximate metal centers, subjects with implications ranging from industrial catalysis to metalloprotein structure and function. [1-22]

The versatility of the RCO_2^- ligand is reflected by the wide range of metal binding modes it can adopt (Figure 2). Up to three transition metal ions have been shown to bind to a single carboxylate ligand; [23] more common is the coordination of one or two metals in structurally distinct ways to one or more of the four available electron lone pairs of the carboxylate anion (Figure 3). Examples of every type of bonding situation shown in Figure 2 can be found in any of several reviews published on the inorganic chemistry of carboxylates. [1-3]

Considering the myriad of biological functions performed by metalloproteins, nature has evolved very few ligands to coordinate metal ions. Of these few types of biological ligands, carboxylates provided by aspartate and glutamate side chains form an important class. A survey [24-47] of representative metalloprotein crystal structure determinations reveals the presence of carboxylates bound to the mono- and polymetallic active sites of numerous functionally significant systems (Table I). Among these biomolecules are proteins that perform electron-transfer (azurin, photosystem I), dioxygen metabolism (superoxide dismutases, hemerythrin, ribonucleotide reductase), and hydrolytic chemistry (holoenolase, carboxypeptidase A), to cite just a few examples. Despite their potential importance, however, the roles of carboxylate coordination to metalloprotein active sites in redox potential attenuation and in mechanisms of catalysis, metalloregulation, and metal ion reconstitution have not been systematically investigated.

We and others have begun to study the structures, physical properties, and basis for functional activity of several carboxylate bound polymetallic proteins by preparing and fully characterizing models of their active sites. [11-22] By using simple carboxylates and the appropriate metal starting ma-

* Correspondence and reprints.

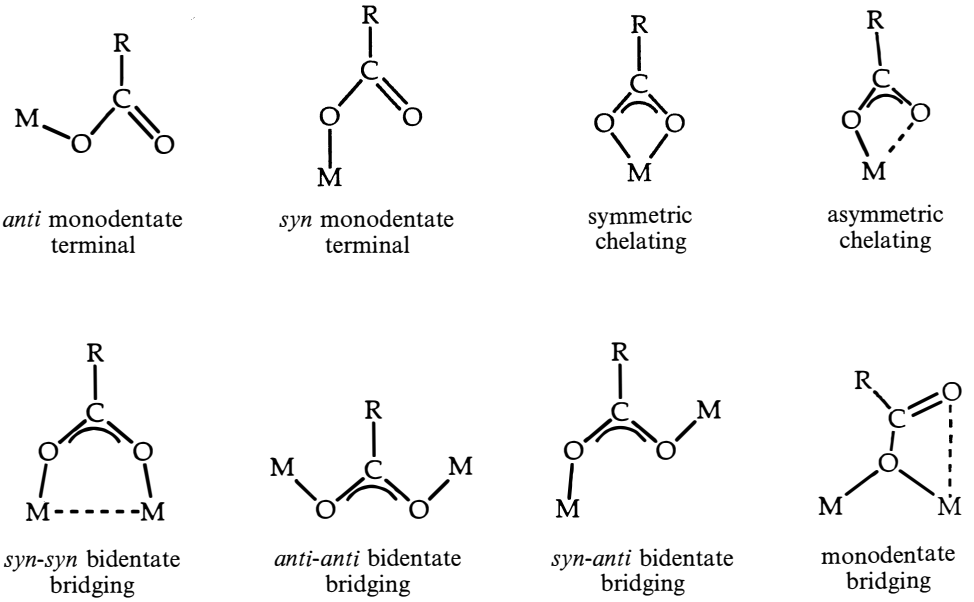

Figure 2. – Carboxylate binding modes in metal complexes.

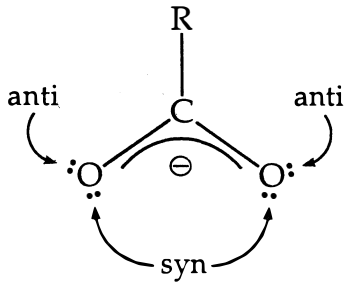

Figure 3. – Schematic of a carboxylate depicting the oxygen *syn* and *anti* lone pairs.

Table I. — Representative structurally characterized metalloproteins with carboxylate coordination at their active sites

Metalloprotein	Function	Active Site Metal(s)	Ref.
Azurin	electron transfer	Cu	24
Superoxide Dismutase	O_2^- detoxification	Cu, Zn	25–26
Carboxypeptidase A	peptide hydrolysis	Zn	27
Thermolysin	thermostable peptide hydrolysis	Zn	28–32
Holoenolase	2-phosphoglycerate dehydration	Zn	33
Lactoferrin	iron binding	Fe	34
Photosystem I Reaction Center	electron transfer	Fe	35–36
Hemerythrin	O_2 transport	Fe	37
Ribonucleotide Reductase	ribonucleotide reduction	Fe	38–39
Superoxide Dismutase	O_2^- detoxification	Fe, Mn	40–41
Concanavalin A	saccharide binding	Mn, Ca	42–43
Trypsin	polypeptide hydrolysis	Ca	44
Phospholipase A_2	phospholipid hydrolysis	Ca	45
Staphylococcal Nuclease	DNA/RNA hydrolysis	Ca	46
Intestinal Ca BP	calcium binding	Ca	47

terial, bidentate carboxylate bridged polynuclear complexes have been assembled, some of which are good structural and spectroscopic metalloprotein core analogs. [11–22,48–55] For the most part, these efforts have focused on complexes of iron and manganese in their higher (greater than +2) oxidation states, prepared in order to model the more accessible forms of polyiron and polymanganese oxo proteins. Recent emphasis on the synthesis of divalent iron and manganese compounds to mimic the less well understood but functionally important reduced forms of these metalloproteins has led to a novel class of molecules that contain a relatively rare monodentate bridging carboxylate. [16,48,56–57] This binding mode is unique in that two metal ions coordinate to a single carboxylate oxygen atom, utilizing both of its available lone pairs. Also distinguishing monodentate bridging from other binding geometries are widely varying interactions of the second, or "dangling", oxygen atom either with one of the bridged metal ions or with a third metal center. The flexibility of this additional metal-oxygen interaction results in significant structural variations within the monodentate bridging carboxylate class of molecules. This phenomenon, which we have termed the "carboxylate shift", [57] identifies the monodentate bridging mode as an important intermediate between other carboxylate orientations.

In this article we present a structural base from which the consequences of the monodentate bridging mode and the carboxylate shift can be assessed. Although, for proteins, monodentate bridging has thus far been definitively identified only in concanavalin A, [42–43] the isolation of a series of synthetic complexes containing such a bridge presages its potential presence in additional metalloproteins and suggests a possible functional role in biology for the carboxylate shift.

Classification of compounds containing monodentate bridging carboxylates

The versatility of carboxylates as metal ligands arises from the presence of four lone pairs of electrons available for metal binding to the carboxylate oxygen atoms. Each lone pair lies in the plane of the carboxylate group and subtends an angle of approximately 120° with respect to the O-C-O

interbond angle. It has been suggested on the basis of stereoelectronic arguments that *syn* lone pairs (*Fig.* 3) are more basic than those in the *anti* positions, [58] and theoretical calculations have supported this idea. [59-60] One consequence of the different relative basicities of the lone pairs is a preferred orientation of carboxylates in proteolytic enzymes to favor *syn* protonation. Protonation of the *syn* electrons is suggested to be $>10^4$ times faster than *anti* protonation in these proteins. [58] This phenomenon has led to the design and synthesis of polycarboxylates structurally constrained to permit interactions of proton donors to *syn* rather than *anti* lone pairs (e. g. **1** in Figure 4) in order to take advantage of

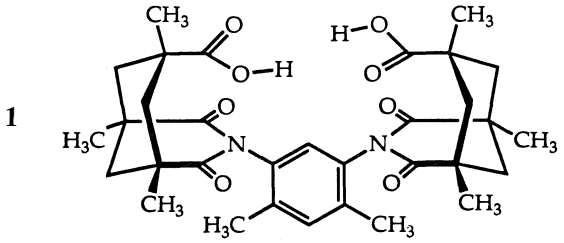

Figure 4. – Schematic of a ligand, **1**, constrained to bind carboxylate syn lone pairs to a metal.

the basicity difference and facilitate molecular recognition. [61] The greater basicity of the *syn* lone pairs also has been used to rationalize preferential *syn* binding of metal ions, a tendency noted in a recent survey of structurally characterized metal-carboxylate complexes, [62] and in the design of highly effective metal chelators. [63] *Syn* lone pair attachment to metals occurs in the most commonly encountered carboxylate binding modes, namely, the monodentate terminal, chelating, and bidentate bridging arrangements (*Fig.* 2). Presumably because of the lower basicity of anti lone pairs, anti monodentate terminal, *syn-anti* bidentate bridging, and *anti-anti* bidentate bridging modes have been less frequently encountered. [1-4]

The monodentate bridging mode is unique in its use of both *syn* and *anti* lone pairs of one oxygen atom in metal binding. This type of bridging was first recognized in polymeric metal carboxylates, where the second oxygen atom interacts with a third metal center to extend the oligomeric array. [23, 64-78] More recently, discrete complexes of divalent Mn, Fe, Co, Cu, Zn and Nb as well as heterometallic systems containing monodentate bridging carboxylates have been reported. [79-101] This class of complexes is generally synthesized by simple treatment of low valent, and often polymeric, metal carboxylates with a mono- or bidentate nitrogen donor ligand. Examination of the results of crystallographic studies of these compounds reveals considerable flexibility in the geometry of the monodentate carboxylate bridge that affords a variety of metal-metal distances and metal coordination geometries, even within a single complex. Analysis of the structural characteristics of discrete compounds containing monodentate bridging carboxylates shows that they can be categorized based on the degree of interaction of the nonbridging, or dangling, oxygen atom with one of the bridged metals. The grouping of complexes in such a manner, while artificial in the sense that there is a continuum of structures, highlights the position of the monodentate bridging orientation as an intermediate between other carboxylate binding modes. Compounds in which the dangling oxygen atom interacts with a third metal, including polymeric materials, have been excluded from this classification scheme. Moreover, no attempt has been made to include all known carboxylate bridged metal complexes in the present analysis.

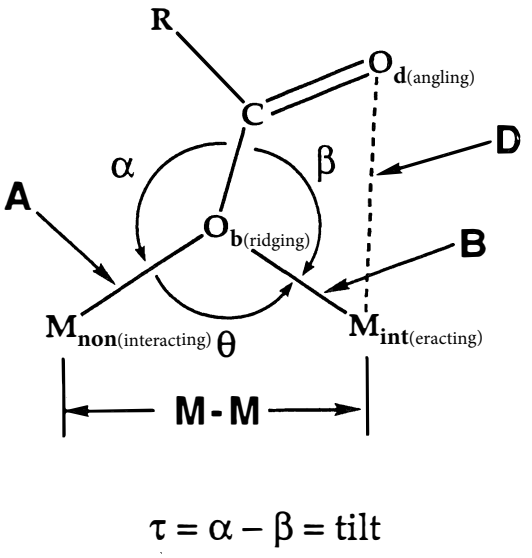

Figure 5. – Structural parameters defining the geometry of monodentate carboxylate-bridged polymetallic centers.

CLASS I: NO OR WEAK INTERACTION

The monodentate bridging carboxylate geometry can be distinguished by several characteristic parameters shown in Figure 5, where *D* is the distance between the dangling oxygen (O_d) and interacting metal (M_{int}), *A* and *B* are the distances along the *anti* and *syn* lone pairs on the bridging oxygen atom (O_b) to the appropriate metal atoms M_{non} and M_{int}, respectively, α and β correspond to the angles between *A* and *B* and the C-O_b distance, and M-M is the metal-metal distance. Complexes having no or only a weak interaction between O_d and one of the bridged metals display several characteristic features, the most obvious being a large *D* value (Table II). Little distortion of the M_{int} geometry is observed as a result of this contact. Class I complexes have short M-M distances arising mainly from shorter A values relative to other complexes having monodentate carboxylate ligands. Another property of these species is a large difference between C-O_d and C-O_b, which indicates localization of the double bond between C and O_d and further supports the fact that the M_{int}-O_d interaction is weak. In some cases, a distinct infrared spectral band occurs in the asymmetric CO_2 stretching frequency region that can be attributed to the localized C=O_d bond, although caution in interpreting such infrared spectroscopic data as evidence for bond localization has been advised. [102]

There is only one complex of which we are aware that contains a monodentate bridging carboxylate with no apparent interaction between O_d and a metal atom. The compound $(Me_4N)[Nb_2Cl_2(tht)(OAc)_5]$ (tht = tetrahydrothiophene; see Figure 6 for a sketch of this and other pertinent ligands), **2**, contains acetate groups bound in three ways: chelating, syn-syn bidentate bridging and monodentate bridging (Figure 7). [79] As is found in some alkaline earth carboxylates, and in contrast to the more commonly encountered positioning of metals in the plane of the carboxylate group, [62] the Nb atoms in **2** lie in a plane perpendicular to that of the monodentate bridging carboxylate. Neither the syn nor the anti lone pairs are directed toward the Nb atoms in this unusual orientation, implying either that rehybridization of the ligating oxygen atom from sp^2+p to sp^3 occurs or that the bonding is primarily ionic. Analogous explanations have been invoked to explain planar rather than pyramidal geometry of coordinated ethers and water molecules to transition

Table II. — Structural parameters for monodentate bridged carboxylate and related complexes. [a]

Complex	*B* (Å)	*D* (Å)	*A* (Å)	M-M (Å)	C-O_b (Å)	C-O_d (Å)	O_b-C-O_d (°)	θ (°)	N_p-M-O_b (°)[b]	β (°)	α (°)	Ref.
						Class I						
(Me_4N) $[Nb_2Cl_2(tht)(OAc)_5]$ (**2**)	2.077 (6)	3.766 (9) 3.875 (9)	2.076 (5)	2.764 (1)	1.36 (1)	1.19 (1)	123.2 (9)	83.4 (2)				79
$[MnZn_2(crot)_6(base)_2]$ (**3**)	1.960 (2)	2.815 (3)	2.238 (2)	3.306 (2)	1.304 (3)	1.211 (3)	121.5 (2)	103.74 (8)	127.91 (7)	113.2 (1)	133.6 (2)	84
$[CoZn_2(crot)_6(base)_2]$ (**4**)	1.993 (3)	2.596 (4)	2.133 (2)	3.325 (2)	1.263 (5)	1.201 (5)	118.9 (4)	107.4 (1)	137.4 (1)	107.8 (2)	137.7 (2)	84
$[NiZn_2(crot)_6(base)_2]$ (**5**)	1.974 (2)	2.570 (3)	2.114 (3)	3.268 (3)	1.287 (6)	1.219 (5)	118.6 (4)	106.0 (1)	138.4 (1)	106.4 (2)	138.3 (2)	84
$[Zn_3(crot)_6(base)_2]$ (**6**)	1.954 (2)	2.752 (3)	2.177 (2)	3.264 (2)	1.306 (3)	1.219 (3)	120.7 (2)	104.26 (9)	130.39 (8)	111.4 (2)	133.7 (2)	84
$[CdZn_2(crot)_6(base)_2]$ (**7**)	1.963 (2)	2.815 (3)	2.314 (2)	3.358 (2)	1.281 (5)	1.209 (5)	121.0 (3)	103.2 (1)	129.4 (1)	114.2 (2)	129.9 (2)	84
anti-$[Fe_3(OAc)_6(BIPhMe)_2]$ (**8**)	2.027 (3)	3.005 (4)	2.151 (3)	3.3251 (9)	1.305 (6)	1.232 (6)	121.1 (5)	105.4 (1)	124.6 (1)	117.3 (3)	137.3 (3)	57
$[Cu_2(hippurate)_4(H_2O)_4]$ (**9**)	1.930 (7)	2.903 (8)	2.372 (7)	3.331 (3)	1.29 (1)	1.21 (1)	123.0 (8)	101.0 (3)		116.5 (6)	142.1 (6)	86
$[Cu_2L(OAc)_2]_n$ (**10**)	1.953 (8)	2.934 (9)	2.496 (5)	3.383 (3)	1.26 (1)	1.21 (1)	124 (1)	98.3 (3)		117.8 (6)	143.8 (7)	87
$[Cu_2(OAc)_3(BIPhMe)_2](BF_4)$ (**11**)	1.952 (5)	3.040 (6)	2.334 (6)	3.257 (2)	1.29 (1)	1.22 (3)	123.6 (8)	98.5 (2)		120.9 (6)	123.6 (5)	88
	1.986 (5)	2.727 (6)	2.432 (6)	3.257 (2)	1.29 (1)	1.23 (1)	122.3 (8)	94.5 (2)		108.7 (5)	143.4 (5)	
$[Cu_2(OAc)_3(bpy)_2]ClO_4$ (**12**)	1.977 (2)	2.716 (2)	2.169 (2)	3.392 (1)	1.319 (4)	1.224 (4)	121.5 (3)	109.8 (1)		108.4 (2)	127.3 (2)	89
						Class II						
anti-$[Mn_3(OAc)_6(BIPhMe)_2]$ (*anti*-**13**)	2.172 (5)	2.488 (7)	2.205 (5)	3.635 (1)	1.28 (1)	1.22 (1)	120.4 (8)	112.3 (2)	142.5 (5)	98.9 (5)	136.1 (5)	57
asym *anti*-$[Mn_3(OAc)_6$ - $(BIPhMe)_2]$ (asym *anti*-**13**)	2.269 (4)	2.306 (5)	2.234 (4)	3.700 (2)	1.269 (8)	1.254 (8)	121.4 (6)	110.5 (2)	163.6 (2)	91.2 (4)	130.2 (4)	95
	2.258 (4)	2.344 (5)	2.238 (9)	3.716 (2)	1.275 (7)	1.246 (8)	120.9 (6)	111.5 (2)	160.9 (2)	92.7 (4)	132.0 (4)	
	2.264 (5)	2.319 (5)	2.240 (5)	3.658 (2)	1.287 (8)	1.239 (8)	120.3 (6)	110.0 (2)	158.3 (2)	91.9 (4)	132.4 (4)	
	2.238 (5)	2.314 (5)	2.248 (5)	3.691 (2)	1.274 (8)	1.252 (8)	119.4 (6)	109.3 (2)	161.0 (2)	93.1 (4)	131.1 (4)	
syn-$[Mn_3(OAc)_6(BIPhMe)_2]$ *syn*-**13**)	2.242 (6)	2.370 (6)	2.181 (6)	3.560 (3)	1.27 (1)	1.25 (1)	119.5 (8)	107.2 (2)	149.3 (2)	94.6 (5)	139.4 (5)	57
	2.138 (6)	2.790 (7)	2.200 (6)	3.370 (3)	1.27 (1)	1.24 (1)	120.9 (9)	101.9 (3)	133.8 (3)	109.4 (6)	147.3 (6)	
syn-$[Mn_3(OAc)_6(phen)_2]$ (**14**)	2.285 (9)	2.425 (6)	2.133 (6)	3.387 (1)	1.263 (9)	1.224 (9)	112.9 (9)	100.1 (3)	137.8 (2)	99.9 (6)	144.9 (6)	94
$[Fe_2(O_2CH)_4(BIPhMe)_2]$ (**15**)	2.113 (2)	2.787 (3)	2.172 (2)	3.5736 (8)	1.270 (4)	1.214 (4)	124.9 (3)	113.0 (1)	146.7 (1)	107.2 (2)	132.1 (2)	56
$[Mn_2(OAc)_3(bpy)_2(ClO_4)]$ (**16**)	2.262 (2)	2.356 (3)	2.160 (3)	3.503 (2)	1.287 (4)	1.239 (5)	120.2 (3)	104.8 (1)		93.0 (2)	136.3 (3)	96
$[Cu_2L_2$ $(OAc)_2]$ (**17**)	1.952 (3)	2.742 (4)	2.445 (3)	3.4452 (7)	1.285 (6)	1.238 (6)	122.2 (5)	102.6 (1)		110.5 (3)	136.3 (3)	90
	1.953 (3)	2.620 (4)	2.650 (3)	3.4452 (7)	1.271 (7)	1.226 (9)	122.4 (6)	95.7 (1)		106.5 (4)	155.3 (4)	
$[Cu_2L_2(OAc)_2]$ (**18**)	1.978 (3)	2.828 (6)	2.512 (5)	3.379 (2)	1.277 (8)	1.235 (9)	123.3 (5)	96.9 (2)		112.6 (4)	150.2 (3)	91
$[Cu_2L_2(OAc)_2]$ (**19**)	1.960 (9)	2.900 (9)	2.498 (8)	3.384 (4)	1.28 (1)	1.24 (2)	124 (1)	98.1 (3)		114.4 (8)	147.1 (8)	92
$[Cu_2L_2(OAc)_2]$ (**20**)	1.987 (4)	2.817 (6)	2.496 (4)	3.542 (3)	1.265 (9)	1.24 (1)	123.7 (7)	103.8 (2)		111.9 (4)	143.4 (4)	97
$[Cu_2L_2(OAc)_2]$ (**21**)	1.976 (2)	2.630 (3)	2.577 (2)	3.4091 (7)	1.268 (4)	1.233 (5)	123.1 (3)	96.06 (7)		105.9 (2)	157.9 (2)	98

Table II (*continued*)

Complex	*B* (Å)	*D* (Å)	*A* (Å)	M-M (Å)	C-O_b (Å)	C-O_d (Å)	O_b-C-O_d (°)	θ (°)	N_p-M-O_b (°)[b]	β (°)	α (°)	Ref.
					Class III							
$[Mn_3(O_2CPh)_6(bpy)_2]$ (**22**)	2.285 (4)	2.274 (4)	2.239 (3)	3.588 (1)	1.284 (6)	1.257 (8)	119.8 (6)	104.9 (2)		90.5 (4)	135.0 (3)	16,96
$[MgZn_2(crot)_6(base)_2]$ (**23**)	2.376 (3)	2.081 (3)	2.057 (3)	3.518 (3)	1.223 (4)	1.249 (5)	118.7 (4)	104.8 (1)	151.71 (9)	85.8 (2)	165.1 (2)	84
$[CaZn_2(crot)_6(base)_2]$ (**24**)	2.836 (3)	1.965 (2)	2.284 (3)	3.855 (3)	1.221 (4)	1.266 (4)	122.6 (3)	97.08 (8)	148.74 (8)	73.0 (2)	190.0 (2)	84
$[SrZn_2(crot)_6(base)_2]$ (**25**)	3.203 (5)	1.930 (3)	2.462 (4)	4.050 (5)	1.213 (7)	1.252 (7)	124.6 (4)	90.3 (1)[c]	144.1 (1)[c]	63.0 (3)	206.8 (4)	84
$[BaZn_2(O_2CCMe_3)_6(base)_2]$ (**26**)	3.079 (6)	1.950 (5)	2.615 (7)	4.224 (2)	1.21 (1)	1.24 (1)	123.5 (8)	95.4 (2)[c]	147.5 (2)[c]	66.7 (5)	198.2 (6)	85
	2.930 (6)	1.965 (6)	2.649 (6)	4.128 (2)	1.23 (1)	1.26 (1)	121.5 (8)	95.3 (2)[c]	148.8 (2)[c]	70.8 (5)	213.3 (6)	
$[Co_3(O_2CPh)_6(base)_2]$ (**27**)				3.559								80–81
$[Co_3(O_2C(C_6H_4NO_2))_6(base)_2]$ (**28**)				3.552								81
$[Fe_2(tpa)_2(OAc)_2](BPh_4)_2$ (**29**)	3.488 (2)	1.998 (1)	2.146 (2)	4.2888 (6)	1.243 (3)	1.267 (3)	125.4 (2)	96.22 (7)[c]		59.4 (1)	138.5 (2)	99
$[Mn_2(OAc)_2(bpy)_4](ClO_4)_2$ (**30**)	3.412 (2)	2.098 (2)	2.112 (2)	4.5832 (8)	1.259 (3)	1.261 (4)	124.1 (2)	109.91 (8)[c]		64.5 (1)	132.7 (1)	96
$[CuL(imH)_2]_2$ (**31**)	3.755 (2)	2.874 (2)	1.939 (1)	5.0295 (4)	1.271 (2)	1.232 (2)	123.7 (2)	120.70 (6)[c]		57.14 (9)	117.2 (1)	100
$[Pb_2(pa)_4(H_2O)]_n$ (**32**)	2.79 (2)	2.51 (2)	2.58 (2)	4.706 (2)	1.26 (4)	1.28 (5)	122 (2)	122.5 (8)[c]		88 (2)	122 (1)	101
$[Cu_2L_2(OAc)_2]$ (**33**)	2.003 (2)	2.604 (3)	2.665 (2)	3.5057 (8)	1.280 (5)	1.236 (5)	123.1 (4)	96.32 (9)		103.7 (2)	159.8 (2)	98
Concanavalin A (ConA)	2.46	2.50	2.28	4.25								42

[a] Refer to Figure 5 for the definition of the structural parameters given in this table and the text and Figure 6 for ligand abbreviations.

[b] N_p refers either to the terminal nitrogen atom or to the nitrogen atom in the trigonal plane in complexes with trigonal bipyramidal metals. See text.

[c] These values are really not applicable since the carboxylate is now syn-syn or syn-anti bidentate bridging.

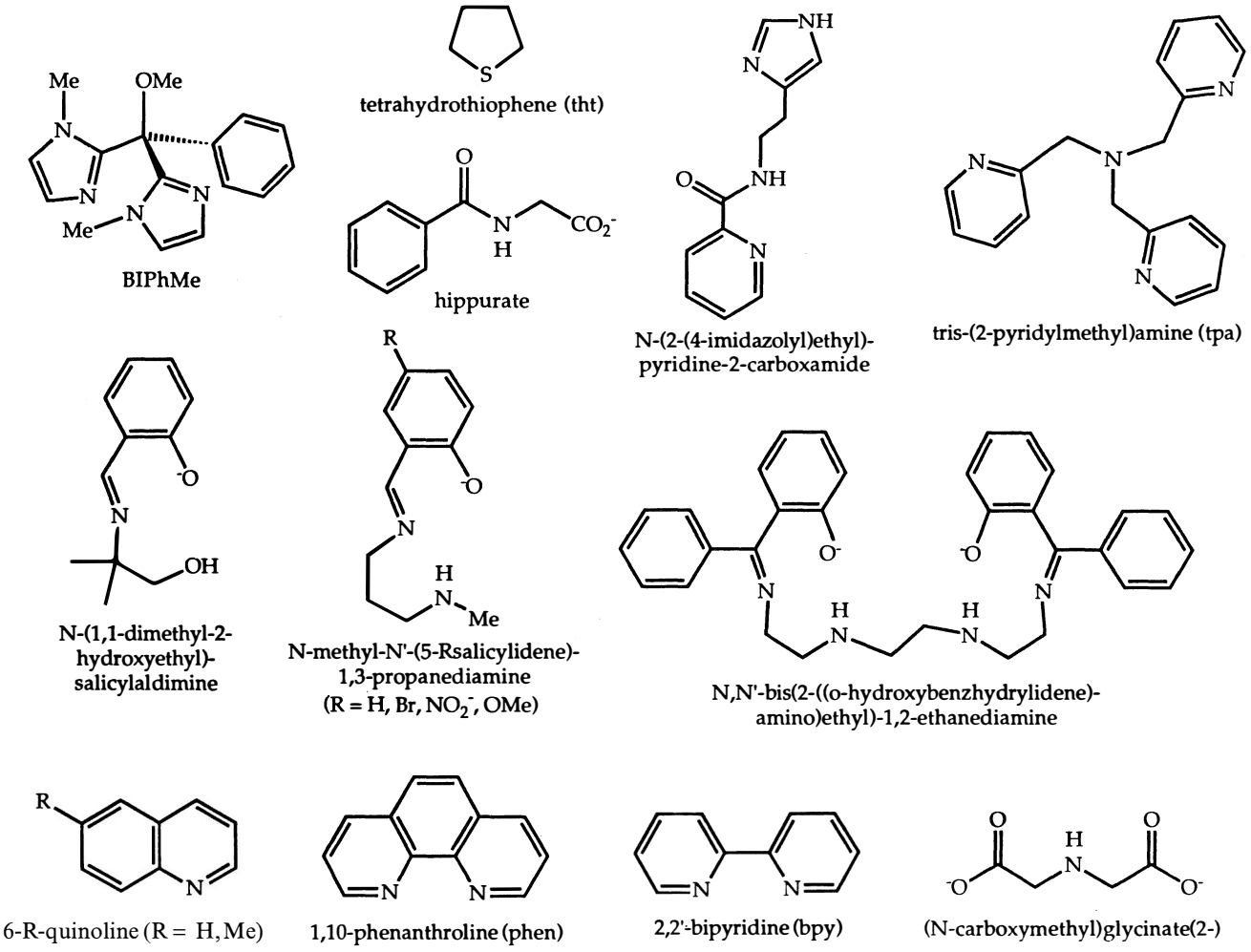

Figure 6. – Ligands.

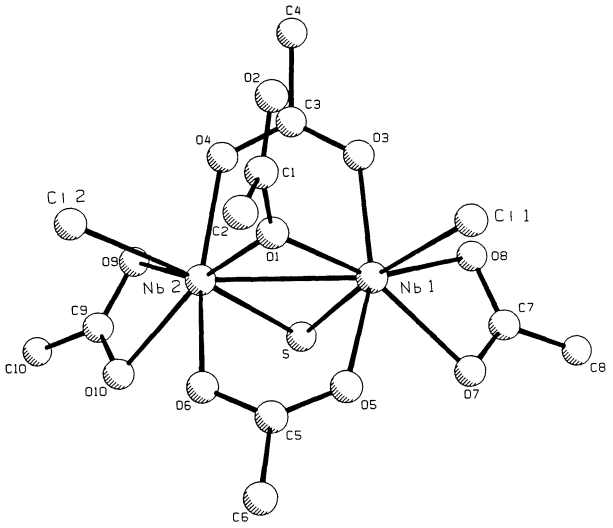

Figure 7. – Structure of the anion of **2**, $[Nb_2Cl_2(tht)(OAc)_5]^-$. For clarity, only the sulfur atom of the tht ligand (Figure 6) is depicted.

metals. [103] There is no interaction between the Nb atoms and O_d, the *D* value being greater than 3.75 Å for both metals (Table II). Consistent with the absence of significant contact between the O_d and Nb atoms is the observation of double bond localization between C and O_d, as revealed by the distances 1.36 (1) Å and 1.19 (1) Å for C-O_b and C-O_d, respectively (Table II). In this case, infrared spectroscopic support for such localization is unequivocal. Two bands appear in the asymmetric CO_2 stretching region of the IR spectrum at 1 523 cm^{-1} and 1 723 cm^{-1}, which can be assigned to the bidentate and monodentate acetate ligands, respectively.

A series of linear homo- and heterotrinuclear complexes consisting of a central hexacoordinate metal flanked by two tetracoordinate Zn^{2+} or Co^{2+} ions was recently reported (Figure 8). [80–85] Each terminal Zn^{2+} or Co^{2+} is connected

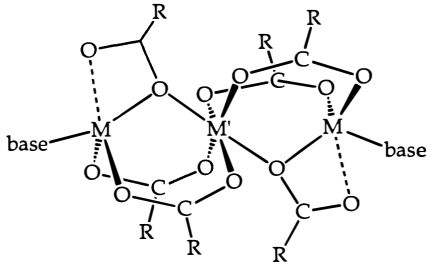

base = quinoline or 6-Me-quinoline

Figure 8. – Generalized structure for $[M_2M'(O_2CR)_6(base)_2]$ complexes **3-7** and **22-28**.

to the central metal by one monodentate and two *syn-syn* bidentate bridging carboxylate ligands. The compounds that contain transition or post-transition metals in the central position and Zn^{2+} in the terminal positions, $[M_2M'(O_2CR)_6(base)_2]$ [R = CH = CHMe, base = quinoline (C_9H_7N),

M = Zn (II) and M′ = Mn (II) (**3**), Co (II) (**4**), Ni (II) (**5**), Zn (II) (**6**) or Cd (II) (**7**)], [84] display only weak interactions between the dangling oxygen atoms and the terminal metals. Support for the presence of some bonding interaction between M_{int} and O_d includes the observed disposition of the carboxylate such that it always places the dangling oxygen near a tetracoordinate terminal metal. In addition, the carboxylate group is tilted in such a way as to bring O_d closer to the terminal metal, as evidenced by the difference (τ, *Fig.* 5) between α and β of up to 32° (Table II). The *D* values are > 2.5 Å in these complexes, however, indicating that the M_{int}-O_d interactions are still rather weak. This interpretation is supported by the relatively short C-O_d bonds (1.201 (5) - 1.219 (5) Å) and the disparity (> 0.06 Å) between C-O_d and C-O_b distances, indicating significant bond localization within the bridging carboxylate (Table II). A distinct band at ca. 1 625 cm^{-1} in the IR spectra of these complexes was assigned as the monodentate carboxylate asymmetric CO_2 stretch based on the bond localization observed in the crystal structures. Another manifestation of the relative strength of the M_{int}-O_d interaction is the distortion of the M_{int} coordination sphere from the tetrahedral geometry expected in the absence of any interaction with the dangling oxygen atom for these compounds. The angle bisected by the M_{int}-O_d vector, O_b-M_{int}-N, where N is the quinoline nitrogen atom, is a reasonable measure of this distortion. Although O_b-M_{int}-N angles range from 128-138° for these complexes (Table II), a significant deviation from the 109.6° characteristic of tetrahedral coordination, these values are still far from the 180° angle expected for the trigonal bipyramidal stereochemistry which these metals approach as the M_{int}-O_d interaction strengthens (vide infra). It is also noteworthy that the angles between the other ligands coordinated to M_{int} range from 99-112°, much closer to the tetrahedral value, again supporting the assignment of the M_{int}-O_d interactions as being weak in these complexes.

Another complex displaying a weak interaction of O_d with one of the bridged metals is $[Fe_3(OAc)_6(BIPhMe)_2]$ [BIPhMe = 2,2′-bis (1-methylimidazolyl)phenylmethoxymethane)], **8** (*Fig.* 9). [57] This complex has a linear structure

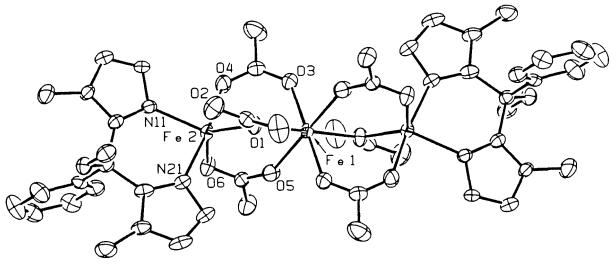

Figure 9. – ORTEP drawing of $[Fe_3(OAc)_6(BIPhMe)_2]$, **8**.

similar to that of the trinuclear complexes described above, except that the terminal metal ions are pentacoordinate in this case. The *D* value of 3.005 (4) Å is one of the longest observed for any complex containing a carboxylate bridging in the monodentate mode, excluding **2** (Table II). The 0.07 Å difference between C-O_d and C-O_b also indicates a weak M_{int}-O_d interaction. Nevertheless, a distinct C = O IR band is not observed for the monodentate acetate ligands in this complex. The terminal Fe^{2+} ions adopt a trigonal bipyramidal coordination geometry. There is very little perturbation of this geometry by interaction with the dangling oxygen atom, as judged by the 124.6 (1)° N_p-Fe-O_b angle (Table II), which is bisected by the Fe_{int}-O_d vector, and the values of the other angles in the trigonal plane, 124.9 (1)° and 110.5 (1)°. [57] The large quadrupole splitting, 3.60 mm s^{-1} versus Fe metal, for the terminal Fe^{2+} ions in the Mössbauer spectrum of this complex is consistent with the inherently less symmetric pentacoordinate environment of the terminal iron atoms relative to the octahedrally coordinated central iron atom. The latter has a quadrupole splitting of 2.64 mm s^{-1}. The monodentate carboxylates tilt toward the terminal metal ions, as indicated by a τ value of 20°, but this distortion is relatively small compared to those observed in other complexes (Table II).

A series of complexes containing a pair(s) of cupric ions bridged asymmetrically by two monodentate carboxylates has been reported. [86-93] Both Cu (II) ions have four ligands, including O_b from one of the bridging carboxylates, bound in a square planar arrangement (*Fig.* 10). Each of the O_b

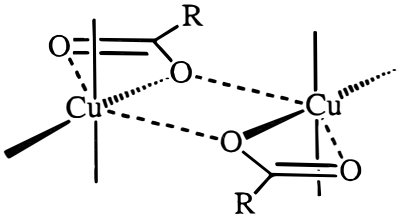

Figure 10. – Schematic representation of dicopper(II) complexes containing two monodentate bridging carboxylates.

atoms, besides bonding at a distance of 1.9-2.0 Å to one Cu(II) ion (Table II), also interacts weakly (distances, 2.4-2.7 Å) at an axial position of the other Cu(II) ion, thus forming an asymmetric bridge. In addition, each O_d atom associates weakly at the second axial position of one of the Cu(II) ions. Two of these compounds, $[Cu_2(\mu\text{-}L)_2L_2(H_2O)_4]$ (L = hippurate, $(C_6H_5)CONHCH_2CO_2^-$), **9**, [86] and $[Cu_2L(OAc)_2]\cdot 2\ CH_3OH$ (L^{2-} = N, N′-bis (2-((*o*-hydroxybenzhydrylidene)amino)ethyl)-1,2-ethanediamine, $C_6H_5(C_6H_4OH)(C{=}N\text{-}(CH_2)_2\text{-}NH\text{-}CH_2\text{-})_2$), **10**·2 CH_3OH (see *Fig.* 6), [87] fall into class I based on their relatively long Cu_{int}-O_d distances. Compound **9** is a discrete dinuclear complex, whereas **10** is polymeric because the hexadentate Schiff base ligand bridges dinuclear units. Compounds **9** and **10** have long Cu_{int}-O_d distances of 2.903 (8) Å and 2.934 (9) Å, respectively. In addition, the C-O_d and C-O_b bonds in **9** differ by 0.08 Å, while a similar difference of 0.05 Å is observed for **10** (Table II). The τ value of ~ 26° in both complexes reveals a lesser tilt of the carboxylate toward the Cu(II) ion with which O_d interacts than in similar dicopper(II) complexes where the Cu_{int}-O_d bonding is stronger (vide infra). In contrast to the previous examples, the metal geometries in these Cu compounds are not distorted by M_{int}-O_d interactions. We attribute this lack of structural reorganization to the fact that movement of O_d is toward the face of the Cu square plane rather than along a polyhedral edge, as was the case for the Fe, Co and Zn complexes discussed above.

Two other dicopper(II) complexes fall naturally into class I. The first of these, $[Cu_2(OAc)_3(BIPhMe)_2](BF_4)\cdot 3\ H_2O$, **11**·3 H_2O, was recently prepared in our laboratory. [88] It contains a triply bridged core comprised of two Cu (II) ions linked by two monodentate bridging acetates and one syn-syn bidentate bridging carboxylate (*Fig.* 11). The core of this complex is similar to those discussed above, except that the bidentate bridging carboxylate bonds to the in-plane positions in both Cu(II) coordination spheres, filling coordination sites occupied by terminal ligands in **9** and **10**. For one of the monodentate carboxylates, having *D* = 3.040 (6) Å, the difference between C-O_d and C-O_b is 0.07 Å (Table II).

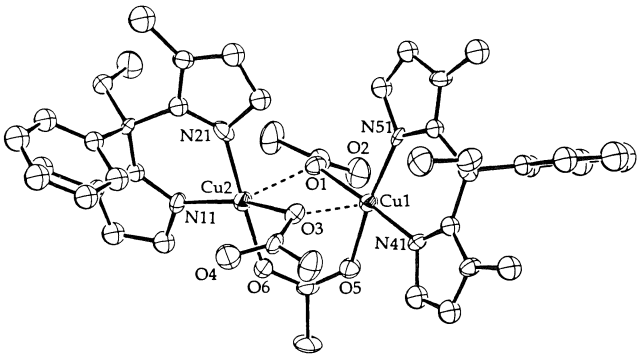

Figure 11. – ORTEP drawing of the cation of **11**, $[Cu_2(OAc)_3(BIPhMe)_2]^+$.

Its τ value, 2.7°, is the smallest observed in any of the monodentate carboxylate bridged complexes and indicates virtually no tilt of the carboxylate toward Cu_{int}. The second monodentate carboxylate in this complex is actually better categorized as a class II ligand, discussed in the next section.

The final class I complex contains two cupric ions bridged by two syn-syn bidentate and one monodentate carboxylate groups, $[Cu_2(OAc)_3(bpy)_2](ClO_4)$ (bpy = 2,2′-bipyridine), **12**, (*Fig.* 12). [89] It has a core structure resembling one half of

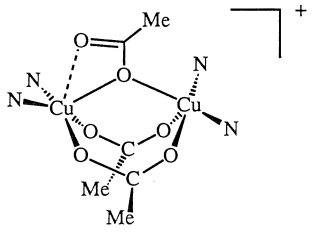

Figure 12. – Schematic representation of the cation of **12**, $[Cu_2(OAc)_3(bpy)_2]^+$.

compounds **3-8**. Although the *D* value of 2.716 (2) Å is shorter than observed for **9-11**, the difference of 0.095 Å between C-O_d and C-O_b and small carboxylate tilt toward Cu_{int} of only 18.9° indicate that there is probably little interaction between Cu_{int} and O_d (Table II).

To summarize, class I complexes display little or no interaction between M_{int} and O_d, as evidenced by several crystallographic parameters. An important structural feature of these complexes is M-M, which ranges from 3.257 (2) Å to 3.39? (1) Å, excluding compound **2**, which has a metal-metal bond (Table II). These values are short in comparison to the M-M values for complexes in classes II and III. Another notable observation is that, for class I complexes, *B* is ~2 Å and less than *A*. The disparity between *A* and *B* dramatically increases in complexes of classes II and III, where the monodentate bridge begins to move toward bidentate bridging or chelating modes, a clear demonstration of the carboxylate shift.

CLASS II: MODERATE INTERACTION

In some complexes containing monodentate bridging carboxylates there is significantly greater interaction between one of the bridged metals and O_d than observed for class I complexes. These compounds can be distinguished from those having fully formed M_{int}-O_d bonds, however. The diminished *D* values that set these complexes apart from class I molecules significantly distort the coordination geometry of M_{int}. In addition, the monodentate carboxylates tend to have more equivalent C-O bond lengths, and M-M is lengthened as a result of an increase in *A* and, in some cases, *B*. A more distinct tilt of the carboxylate toward M_{int} is observed in such class II complexes. Finally, considerable variability in the geometry of the carboxylate-bridged dimetallic unit occurs as the M_{int}-O_d interaction strengthens. As a consequence, some interesting correlations can be drawn.

Among class II compounds are two linear, trinuclear Mn(II) complexes that are structurally similar to **3-7** and **8**, namely, $[Mn_3(OAc)_6(BIPhMe)_2]$, **13**, [57] and $[Mn_3(OAc)_6(phen)_2]$ (phen = 1,10-phenanthroline), **14**. [94] Characterization of three different crystal forms of **13** by X-ray diffraction [57, 95] revealed the presence of at least two isomers, designated *syn*- and *anti*-**13** depending upon the disposition of BIPhMe imidazole groups with respect to the best plane passing through the three metal atoms and two monodentate oxygen atom bridges (*Fig.* 13). The *anti* isomer of **13** crystal-

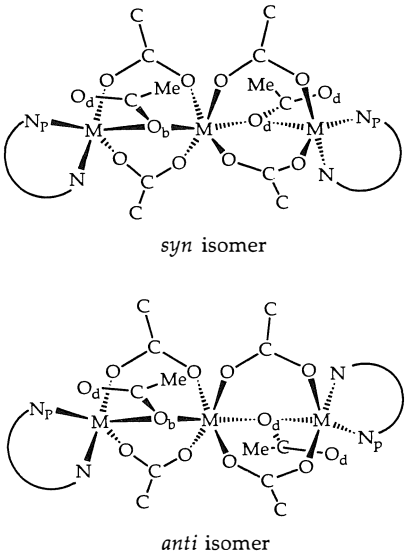

Figure 13. – Schematic representation of *syn*- and *anti*-forms of **8** and **13-14**, where N_P is the nitrogen atom in the trigonal plane of the terminal metal ions.

lizes in both centrosymmetric [57] and asymmetric forms, [95] while only an asymmetric form of the *syn* isomer exists. [57] Compound **14** crystallizes as the *syn* isomer, the two halves of the molecule being related by a C_2 axis passing through the central Mn(II) ion. A dinuclear Fe(II) complex, $[Fe_2(O_2CH)_4(BIPhMe)_2]$ (**15**), [56] and a dinuclear Mn(II) complex, $[Mn_2(OAc)_3(bpy)_2(ClO_4)]$ (**16**), [96] with cores that resemble one half of the cores of **7** and **13-14**, respectively, can also be categorized in class II.

Compounds **13-16** have *D* values ranging from 2.306 (5) Å to 2.790 (7) Å (Table II). Significant distortion of the M_{int} coordination sphere is evident from the N-M_{int}-O_b angle bisected by the M_{int}-O_d vector and in the trigonal plane of the pentacoordinate M_{int} atom. The N-M_{int}-O_b angles, which range from 133.8 (3)° to 163.6 (2)°, are distorted from the trigonal bipyramidal value of 120° toward the octahedral angle of 180°, owing to the stronger interaction between M_{int} and O_d. The N-M_{int}-O_b angle correlates in roughly a linear fashion with *D*. Furthermore, there is an approximately linear correlation between *D* and *B* for **13-16** (*Fig.* 14). The increase

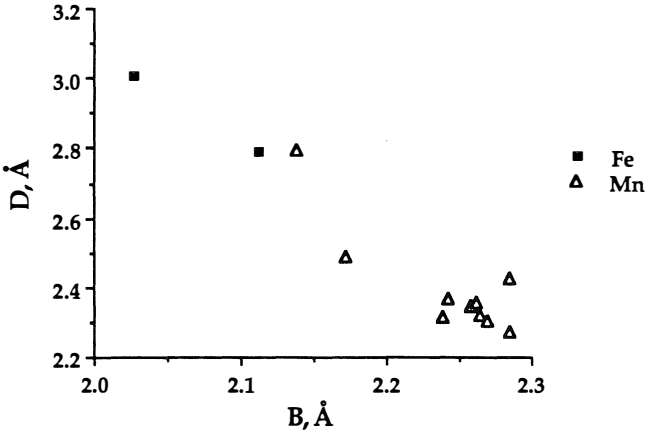

Figure 14. – Plot of D versus B for **8**, **13-16** and **22**.

in *B* that accompanies the decrease in *D* results in a relative lengthening of M-M, which ranges from 3.370 (3) Å to 3.716 (2) Å for **13-16**. Note that both extremes of M-M occur in the same complex, **13**, demonstrating the flexibility afforded by the monodentate bridging carboxylate group. This M-M variation in complexes with similar topologies suggests that caution should be used in interpreting metalloprotein EXAFS data, where structural conclusions are sometimes drawn solely on the basis of metal-metal distances. [104] Moreover, the difference between M_{non}-O_b-C and M_{int}-O_b-C is roughly 40° for **13** and **14**, indicating a marked tilt of the carboxylate toward M_{int}. Compared to the values for **13** and **14**, the tilt of the carboxylate toward M_{int} is much smaller ($\tau = 24.9°$) in **15**. The carboxylate ligands display more symmetrical internal bonding in **13-16** as reflected by differences of $\leqslant 0.06$ Å between C-O_b and C-O_d, indicating greater delocalization of the double bond.

The Cu(II) complexes $[Cu_2(OAc)_2(L)_2]$ [LH = N-(1,1-dimethyl-2-hydroxyethyl)salicylaldimine (**17**), [90] LH = N-methyl-N′-salicylidene-1,3-propanediamine (**18**), [91] LH = N-methyl-N′-(5-methoxysalicylidene)-1,3-propanediamine (**19**), [92] LH = N-(2-(4-imidazolyl)ethyl)pyridine-2-carboxamide (**20**) [97] or LH = N-methyl-N′-(5-nitrosalicylidene)-1,3-propanediamine (**21**); [98] see *Fig.* 6] are similar in basic structure to **9** and **10** (*Fig.* 10). Complexes **18-20** can be readily assigned to class II while only one of the monodentate carboxylates in **17** falls into this category and complex **21** lies somewhat closer to class III. closer to class III. One of the monodentate carboxylates of **11** also best fits into class II. Less marked differences between classes I and II are observed for Cu(II) than for Mn(II) and Fe(II). In fact, the change in M-M distance is insignificant for **11**, **17-19** and **21** relative to **9** and **10** (Table II). This decoupling of M-M from *D* parameters probably results from the weaker link between metals provided by the asymmetrically bridging carboxylate. There is also relatively little change in *B* as *D* decreases. A smaller *D*, less asymmetry in the carboxylate group and a larger tilt of the monodentate carboxylate toward M_{int} are the characteristics that distinguish **11** and **17-21** from class I complexes **9** and **10**.

The overall distinction between classes I and II can be seen most clearly by comparing the cores of **8** and **15** (*Fig.* 15), As *D* decreases M-M increases. The strengthening of the M_{int}-O_d interaction in **15** (class II) compared to **8** (class I) is reflected by a greater tilt of the carboxylate toward M_{int}, an increase in the ratio of the distances *D* and *B*, and a significantly more distorted trigonal bipyramidal geometry about M_{int}. The effect of the stronger M_{int}-O_d interaction is essentially movement of the carboxylate from monodentate bridging toward bidentate bridging. This type of motion illustrates one aspect of the carboxylate shift, depicted in Figure 16, the ramifications of which are further discussed in the next section. It is interesting that, in the Cu(II) complexes, no significant correlation of *B* with *D* is observed. We visualize this movement as being toward a non-bridging chelating interaction of the carboxylate with M_{int}, further extending the carboxylate shift concept (*Fig.* 16). Class II thus affords an important transition between the weak interactions of M_{int} and O_d in class I and the strong interactions observed in class III.

CLASS III: STRONG INTERACTION

We define class III complexes as those having a strong interaction between M_{int} and O_d, delineated by small *D* values. There are two variants here, namely, the cases where $B > D$ and where $A \geqslant D$. The former is represented by complexes that have shifted toward syn-syn bidentate bridging as *D* decreases and *B* increases, while the latter represents a shift toward chelate formation as *D* decreases and *A* increases. These movements generally lead to larger M-M values than observed for class II complexes and an even greater tilt of the carboxylate group toward M_{int}.

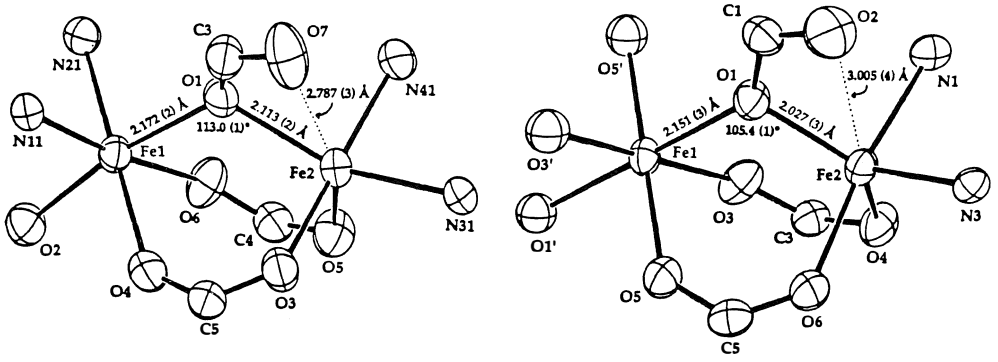

$[Fe_2(O_2CH)_4(BIPhMe)_2]$

Fe···Fe 3.574 (1) Å

N31-Fe2-O1 146.7 (1)°

$[Fe_3(OAc)_6(BIPhMe)_2]$

Fe···Fe 3.325 (1) Å

N3-Fe2-O1 124.6 (1)°

Figure 15. – ORTEP drawings comparing the cores of **8** and **15**.

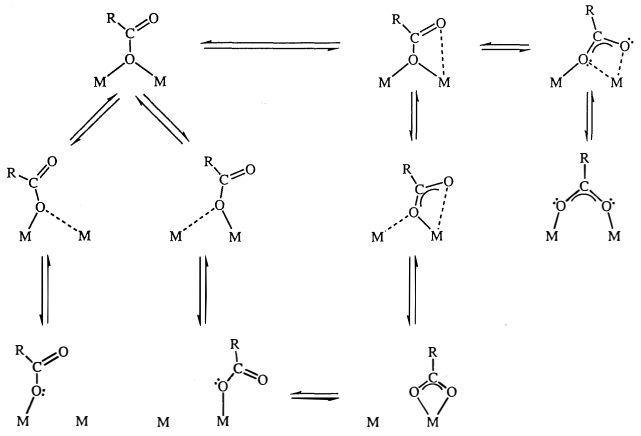

Figure 16. – The "carboxylate shift".

A linear trinuclear Mn(II) complex, $[Mn_3(O_2CPh)_6(bpy)_2]$ (**22**), similar in structure to **8** and **13-14**, was reported recently. [16, 96] The *D* values in **22** are 0.011 Å less than the *B* values for the complex (Table II), placing it very close to the border between classes II and III. In fact, some of the other structural parameters, including the M-M distance and τ, are in the ranges observed for the class II complexes **13-14**. In complex **22**, as in **8** and **13-16**, *D* is correlated with *B* (*Fig.* 14). It is interesting that linear trinuclear complexes of this stoichiometry (**8**, **13-14** and **22**) span all three classes, further demonstrating the flexibility of this structural unit.

Complexes similar to **3-7** (*Fig.* 8), but with alkaline earth metals in the central position [84–85] or Co^{2+} in all three positions, [80–81] $[M_2M'(O_2CR)_6(base)_2]$ [$M=Zn^{2+}$, $M'=Mg^{2+}$, base = quinoline, C_9H_7N, R = CH = CHMe (**23**); $M=Zn^{2+}$, base = 6-methylquinoline, $C_{10}H_9N$, R = CH = CHMe, $M'=Ca^{2+}$ (**24**) or Sr^{2+} (**25**); $M=Zn^{2+}$, $M'=Ba^{2+}$, base = quinoline, $R=CMe_3$ (**26**); $M=M'=Co^{2+}$, base = quinoline, $R=C_6H_5$ (**27**) or $R=C_6H_5NO_2$ (**28**)], exhibit *D* values that are 0.295-1.273 Å shorter than the corresponding *B* values. These results demonstrate the movement of the monodentate carboxylate to a *syn-syn* bidentate bridging mode (*Fig.* 16, Table II). In **25** and **26**, the formerly monodentate carboxylates are indistinguishable from the other bridging ligands. The M-M distances, 3.518 (3) Å to 4.224 (2) Å, are significantly extended relative to the values observed for **3-7**. As the interaction between M_{int} and O_b weakens, the M_{int} geometry moves once again toward tetrahedral, analogous to the case where *D* is long, as in class I complexes. The τ value increases as the central metal varies from Mg^{2+} to Ba^{2+}, reflecting the tilt of the carboxylate into a *syn-syn* bidentate bridging mode.

A key aspect of the shift from the monodentate to *syn-syn* bidentate bridging mode is the transition of the O_b lone pair donation to M_{non} from *anti* to *syn*. In fact, the immediate result of a decrease in *D* and increase in *B* without reorientation of O_b relative to M_{non} is a *syn-anti* bidentate bridging carboxylate. This rare binding mode has been observed recently in three discrete complexes, $[Fe_2(tpa)_2(OAc)_2](BPh_4)_2$ [**29**; tpa = tris-(2-pyridylmethyl)amine], [99] $[Mn_2(OAc)_2(bpy)_4](ClO_4)_2$ (**30**) [96] and $[CuL(imH)_2]_2$ [**31**; L = (N-carboxymethyl)glycinate(2-), imH = imidazole], [100] all of which contain a dimetallic center spanned solely by two *syn-anti* carboxylates (*Fig.* 17). A polymeric Pb(II) complex of phenoxyacetate (pa), $[Pb_2(pa)_4(H_2O)]$, **32**, [101] also contains such a *syn-anti* bridging carboxylate. Examination of the M-M values for **29-32** (Table II) reveals that *syn-anti* bridges

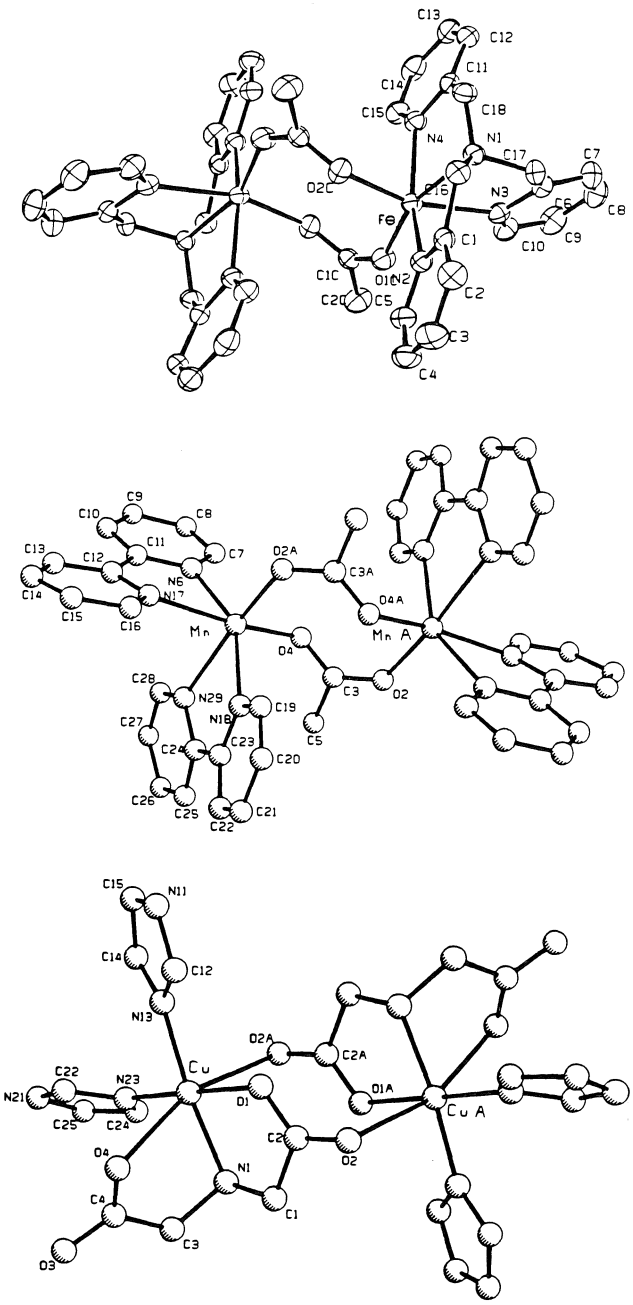

Figure 17. – Structures of the dications of **29**, $[Fe_2(OAc)_2(tpa)_2]^{2+}$ (top), and **30**, $[Mn_2(OAc)_2(bpy)_4]^{2+}$ (middle), and the neutral complex **31**, $[Cu_2L_2(ImH)_4]$ (bottom).

yield an expanded dimetallic center relative to other carboxylate bridging modes. This result makes it less likely that a *syn-anti* bridging carboxylate occurs as an intermediate between monodentate and *syn-syn* bidentate bridging carboxylates in metalloproteins, where the space required for such an expansion of a dimetallic center might be limited. On the other hand, if such a transformation were to take place, it might trigger considerable protein chain movement and possibly be linked to substrate binding or release, redox potential changes, or to allosterism. Most probably, the presence of other bridging ligands would add rigidity to the core, allowing the monodentate to *syn-anti* to *syn-syn* transitions to occur without the large increase in M-M seen in **29-32**. Complex **24** contains a monodentate carboxylate poised close to the *anti/syn* transition, as indicated by the nearly linear M_{non}-O_b-C

angle of 190.0 (2)° (Table II). Again, as in complex **2**, the metal ion appears not to be bound directly to either the *syn* or *anti* lone pairs of the carboxylate. In this case, such an orientation may be a consequence of either rehybridization of O_b or of a more ionic alkali earth M_{non}-O_b bond. [62, 103] The basis for such unusual orientations remains unclear and would be an interesting topic for theoretical investigation. In any case, the M-M distance of 3.855 (3) Å in **24** suggests that such a linear arrangement could possibly exist as an intermediate in the movement from monodentate to *syn-syn* bidentate bridging, precluding the need for a dimetallic center to pass through a fully extended *syn-anti* bridged state during such motion.

Further shift of the carboxylate ligand toward chelate formation as *D* decreases and *A* increases occurs in the dicopper complex $[Cu_2L_2(OAc)_2]$ [LH = N-methyl-N′-(5-bromosalicylidene)-1,3-propanediamine (**33**)] [98] and in one of the monodentate carboxylates of **17** (*Fig.* 10). In these cases, *D* has decreased to a point where it is less than *A*, which in turn is somewhat larger than the *A* values observed for the other dicopper (II) complexes discussed. As a result, M-M is also larger in **17** and **33** (Table II). A more significant tilt of the carboxylate toward M_{int} is observed, as evidenced by a difference of ~50° between M_{int}-O_b-C and M_{non}-O_b-C.

In sum, the geometries of the class III complexes nicely illustrate the link between the monodentate bridging, *syn-anti*/*syn-syn* bidentate bridging, and chelate binding modes of carboxylate ligands and thus provide the basis for the carboxylate shift (*Fig.* 16).

Factors Affecting the Carboxylate Shift and its Possible Biological Relevance

A common feature among the growing list of complexes that contain a monodentate bridging carboxylate is the presence of relatively low oxidation state metal ions. In no instance to date does a carboxylate use a single oxygen atom to bridge two metals that have oxidation states greater than +2, even when higher redox levels are readily accessible (e. g. for iron and manganese). This preference for monodentate linking of low valent metal ions presumably derives from resonance stabilization and effective charge delocalization in the carboxylate anion. The formal charge on a carboxylate oxygen atom linking two metal centers ($-^1/_2$) is less than that of oxo (-2), alkoxo (-1), aryloxo (-1), and hydroxo (-1) ligands, all of which form stable bridges between higher valent metals such as Fe(III), Mn(III) and Mn(IV). [11–22, 105] In effect, the monodentate carboxylate bridge offers a "softer" ligand than the other oxygen atom donors and thus is particularly well-suited for bridging mono- and divalent metal ions.

The strength of the M_{int}-O_d interaction does not appear to correlate with the electron density or geometrical preferences of M_{int}. The factors responsible for differences in this interaction are clearly subtle, as evidenced by the observation of varying monodentate carboxylate geometries in the isomeric series of *syn*/*anti*-$[Mn_3(OAc)_6(BIPhMe)_2]$ complexes.

An important manifestation of an increased dangling oxygen atom interaction is movement of the monodentate bridging carboxylate, a carboxylate shift, toward either chelating terminal or bidentate bridging orientations (*Fig.* 16). The ability of a carboxylate ligand to adopt such a continuum of static conformations between different modes in a range of structurally characterized complexes implies that the shift may also be a kinetically important phenomenon. [106] Oxidation of the metal(s) in a dinuclear complex bridged by a monodentate carboxylate would be anticipated to facilitate the shift and allow either separation of the metals or the insertion of a harder, more negatively charged bridge such as oxide or hydroxide. A reaction of this sort has, in fact, been discovered for **15**, which upon exposure to dioxygen forms the (μ-oxo)diiron(III) complex **34** (*Fig.* 18). [48, 56] We

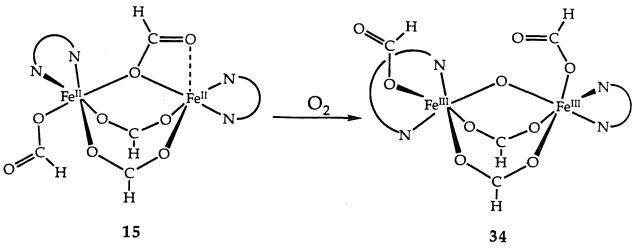

Figure 18. – Conversion of **15** to **34** upon treatment with O_2.

speculate that, in this instance, the monodentate bridging formate in **15** becomes a monodentate terminal ligand in the oxidized product, although supporting evidence such as might be provided by labeling experiments is not yet available. While other types of carboxylate linkage isomerizations have been observed in mononuclear complexes, e. g. between chelating terminal and monodentate terminal, [107] we believe the carboxylate shift in dinuclear complexes to have unique ramifications for dinuclear metalloprotein active sites.

In particular, the facile self-assembly of compounds with monodentate carboxylate bridges between such biologically relevant metals as Mn, Fe, Cu, and Zn suggests to us that such a structural unit may be present and functionally important in nature. A monodentate carboxylate provided by glutamate or aspartate side chains would be a stable alternative to hydroxo or aqua bridges between low valent metals in proteins, especially when a hydrophobic environment is required. Such a bridge has been identified so far only in concanavalin A (ConA). [42–43] ConA is a lectin from jackbeans that binds polysaccharides, presumably at or near a site containing linked Mn(II) and Ca(II) ions (*Fig.* 19). A

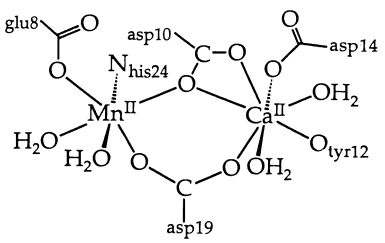

Figure 19. – Structure of concanavalin A (conA).

form of the protein with two Mn(II) ions has also been prepared. [108] A 1.75 Å resolution X-ray crystal structure of conA indicates that the metals in the native system are 4.25 Å apart and are bridged by bidentate and monodentate carbox-

ylates. The latter falls into Class III because of its strong M_{int}-O_d dangling oxygen interaction (Table II). [42]

While significant evidence supports the presence of hydroxo (or aqua) bridges in hemocyanin [109] and the reduced forms of hemerythrin, [110–115] the ligand environments surrounding the low valent metal ions in several other dinuclear metalloprotein active sites are presently unknown. Intriguing possibilities are ribonucleotide reductase (RR) and methane monooxygenase (MMO), both of which are believed to have predominantly oxygen donor ligands about their diiron(II) active sites. [116–119] A recent X-ray structural study of the native (μ-oxo)diiron(III) form of RR has revealed the presence of four carboxylates bound to the core, one bidentate bridging, one chelating, and two monodentate terminal (*Fig.* 20). [38] The reduced diferrous form appears to play a

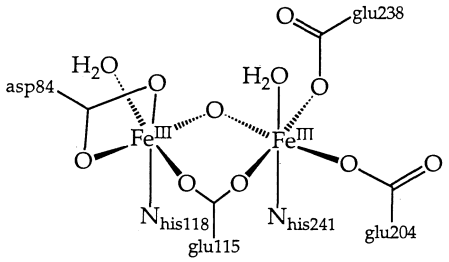

Figure 20. – Structure of the oxidized form of ribonucleotide reductase (RR).

key role in regulation of RR activity, since the native diferric core and the tyrosyl radical necessary for enzymatic catalysis of ribonucleotide reduction are produced in a reaction involving O_2 and the reduced active site. [39] The similarity between aspects of the conversion of **15** to **34** and the generation of active RR according to equation 1 (stoichiometry currently unknown) suggested to us the possible occurrence of a monodentate carboxylate bridge in the reduced form of RR. As shown in Figure 20, glu 238 is positioned *cis* to the oxo bridge in the oxidized core of the protein, poised to replace the oxo ligand and form a monodentate carboxylate bridge upon reduction to the diferrous form. The reverse of this carboxylate shift may occur during the oxidative process of tyrosyl radical generation. Future detailed structural work will allow evaluation of this proposal.

$$\mathrm{Fe(II)_2 + O_2 + tyr\text{-}OH \rightarrow Fe(III)\text{-}O\text{-}Fe(III) + tyr\text{-}O\cdot} \quad (1)$$

Other resonance stabilized, biologically relevant oxyanionic ligands such as phosphate [120] and sulfate [121] also exhibit versatility in the manner in which they bind metal ions. Specifically, phosphate geometries approaching monodentate bridging, analogous to those observed for carboxylates, have been reported. [122] The structural principles that we have employed in our analysis of the metal binding of carboxylates may be similarly applied to their P- or S-based analogues. Consequently, a corresponding "phosphate shift" or "sulfate shift" may have structural and/or mechanistic significance in polymetallic proteins such as purple acid phosphatase [13b, 123] or the recently reported thiosulfate oxidizing protein. [124] Thus, flexibility in the monodentate bridging of metal atoms by phosphate and sulfate anions may parallel that which we have delineated herein for carboxylates, with similarly significant ramifications in biological systems.

Acknowledgment

This work was supported by a grant from the National Institute of General Medical Sciences. R.L.R. is grateful to the NIH for support under Training Grant CA-09112 and W.B.T. to the American Cancer Society for a postdoctoral fellowship. We also thank Professors L. Que, Jr., and G. Christou for kindly supplying unpublished data and preprints of their work prior to publication and J. Rebek for commenting on the manuscript.

REFERENCES

[1] Mehrotra R. C., Bohra R., "*Metal Carboxylates*", Academic, New York, 1983.
[2] Oldham C., *Prog. Inorg. Chem.*, 1968, **10**, 223.
[3] Catterick J., Thornton P., *Adv. Inorg. Chem. Radiochem.*, 1977, **20**, 291.
[4] Cotton F. A., Walton R. A., *"Multiple Bonds Between Metal Atoms"*, Wiley, New York, 1982.
[5] Kitajima N., Fukui H., Moro-oka Y. J., *J. Chem. Soc. Chem. Commun.*, 1988, 485.
[6] Barton D. H. R., *Aldrichim. Acta*, 1990, **23**, 3 and references therein.
[7] Fish R. H., Fong R. H., Vincent J. E., Christou G., *J. Chem. Soc. Chem. Commun*, 1988, 1504.
[8] Murch B. P., Bradley F. C., Que L. Jr., *J. Am. Chem. Soc.*, 1986, **108**, 5027.
[9] Vincent J. B., Huffman H. C., Christou G., Li Q., Nanny M. A., Hendrickson D. N., Fong R. H., Fish R. H., *J. Am. Chem. Soc.*, 1988, **110**, 6898.
[10] Ito S., Inoue K., Matsumoto M., *J. Am. Chem. Soc.*, 1982, **104**, 6450.
[11] (*a*) Lippard S. J., *Angew. Chem. Int. Ed. Engl.*, 1988, **27**, 344; (*b*) Lippard S. J., *Chem. Br.*, 1986, 222.
[12] Kurtz D. M. Jr., *Chem. Rev.*, 1990, **90**, 585.
[13] (*a*) Que L. Jr., True A. E., *Prog. Inorg. Chem.*, 1990, **38**, 97; (*b*) Que L. Jr., Scarrow R. C., *"Metal Clusters in Proteins"* (*A.C.S. Symp. Ser.*, 372), Que L. Jr. Ed., American Chemical Society, Washington, DC, 1988, 152.
[14] Wilkins P. C., Wilkins R. G., *Coord. Chem. Rev.*, 1987, **79**, 195.
[15] Wieghardt K., *Angew. Chem. Int. Ed. Engl.*, 1989, **28**, 1153.
[16] Vincent B., Christou G., *Adv. Inorg. Chem. Radiochem.*, 1989, **33**, 197.
[17] Christou G., *Acc. Chem. Res.*, 1989, **22**, 328.
[18] Brudvig G. W., Crabtree R. H., *Prog. Inorg. Chem.*, 1989, **37**, 99.
[19] Brudvig G. W., Beck W. F., de Paula J. C., *Ann. Rev. Biophys. Biophys. Chem.*, 1989, **10**, 25.
[20] Christou G., Vincent J. B. in *"Metal Clusters in Proteins"* (*A.C.S. Symp. Ser.*, 372), Que L. Jr. Ed., American Chemical Society, Washington, D.C., 1988, 238.
[21] Brudvig G. W., *"Metal Clusters in Proteins"* (*A.C.S. Symp. Ser.*, 372), Que L. Jr. Ed., American Chemical Society, Washington, D.C., 1988, 221.
[22] Renger G., *Angew. Chem. Int. Ed. Engl.*, 1987, **26**, 643.
[23] Mounts R. D., Ogura T., Fernando Q., *Inorg. Chem.*, 1974, **13,** 802.
[24] Norris G. E., Anderson G. F., Baker E. N., *J. Am. Chem. Soc.*, 1986, **108**, 2784.
[25] Tainer J. A., Getzoff E. D., Richardson J. S., Richardson D. C., *Nature*, 1983, **306**, 284.
[26] Tainer J. A., Getzoff E. D., Beem K. M., Richardson J. S., Richardson D. C., *J. Mol. Biol.*, 1982, **160**, 181.
[27] Christianson D. W., Lipscomb W. N., *Acc. Chem. Res.*, 1983, **22**, 62.
[28] Tronrud D. E., Holden H. M., Matthews B. W., *Science*, 1987, **235**, 571.
[29] Tronrud D. E., Monzingo A. F., Matthews B. W., *Eur. J. Biochem.*, 1986, **157**, 261.

[30] Monzingo A. F., Matthews B. W., *Biochemistry*, 1984, **23**, 5724.
[31] Holmes M. A., Tronrud D. E., Matthews B. W., *Biochemistry*, 1983, **22**, 236.
[32] Holmes M. A., Matthews B. W., *J. Mol. Biol.*, 1982, **160**, 623.
[33] Lebioda L., Stec B., *J. Am. Chem. Soc.*, 1989, **111**, 8511.
[34] Anderson B. F., Baker H. M., Dodson E. J., Norris G. E., Rumball S. V., Waters J. M., Baker E. N., *Proc. Natl. Acad. Sci.* (*U.S.A.*), 1987, **84**, 1769.
[35] Deisenhofer J., Epp O., Miki K., Huber R., Michel H., *Nature*, 1985, **318**, 618.
[36] Allen J. P.. Feher G., Yeates T. O., Rees D. C., Deisenhofer J., Michel H., Huber R., *Proc. Natl. Acad. Sci.* (*U.S.A.*), 1986, **83**, 8589.
[37] Sheriff S., Hendrickson W. A., Smith J. L., *J. Mol. Biol.*, 1987, **197**, 273 and references therein.
[38] Nordlund P., Sjöberg B.-M., Eklund H., *Nature*, 1990, **345**, 593.
[39] Stubbe J., *J. Biol. Chem.*, 1990, **265**, 5329 and references therein.
[40] Stallings W. C., Pattridge K. A., Strong R. K., Ludwig M. L., *J. Biol. Chem.*, 1985, **260**, 16424.
[41] Stoddard B. L., Howell P. L., Ringe D., Petsko G. A., *Biochemistry*, 1990, **29**, 8885.
[42] Hardman K. D., Agarwal R. C., Freiser M. J., *J. Mol. Biol.*, 1982, **157**, 69.
[43] Lin S.-L., Stern E. A., Kalb (Gilboa) A. J., Zhang Y., *Biochemistry*, 1990, **29**, 3599.
[44] Bode W., Schwager P., *J. Mol. Biol.*, 1975, **98**, 693.
[45] Dijkstra B. W., Kalk K. H., Hol W. G. J., Drenth J., *J. Mol. Biol.*, 1981, **147**, 97.
[46] Cotton F. A., Hazen E. E. Jr., Legg M. J., *Proc. Natl. Acad. Sci.* (*U.S.A.*), 1979, **76**, 2551.
[47] Szebenyi D. M. E., Obendorf S. K., Moffat K., *Nature*, 1981, **294**, 327.
[48] Tolman W. B., Liu S., Bentsen J. G., Lippard S. J., *J. Am. Chem. Soc.*, 1991, **113**, 152.
[49] Beer R. H., Tolman W. B., Bott S. G., Lippard S. J., *Inorg. Chem.*, 1989, **28**, 4557.
[50] Gomez-Romero P., Casan-Pastor N., Ben-Hussein A., Jameson G. B., *J. Am. Chem. Soc.*, 1988, **110**, 1988.
[51] Feng X., Bott S. G., Lippard S. J., *J. Am. Chem. Soc.*, 1989, **111**, 8046.
[52] Yan S., Que L. Jr., Taylor L. F., Anderson O. P., *J. Am. Chem. Soc.*, 1988, **110**, 5222.
[53] Yan S., Cox D. D., Pearce L. L., Juarez-Garcia C., Que L. Jr., Zhang J. H., O'Connor C. J., *Inorg. Chem.*, 1989, **28**, 2507.
[54] Borovik A. S., Que L., Jr., *J. Am. Chem. Soc.*, 1988, **110**, 2345.
[55] Borovik A. S., Hendrich M. P., Holman T. R., Münck E., Papaefthymiou V., Que L. Jr., *J. Am. Chem. Soc.*, 1990, **112**, 6031.
[56] Tolman W. B., Bino A., Lippard S. J., *J. Am. Chem. Soc.*, 1989, **111**, 8522.
[57] Rardin R. L., Bino A., Poganiuch P., Tolman W. B., Liu S., Lippard S. J., *Angew Chem. Int. Ed. Engl.*, 1990, **29**, 812.
[58] Gandour R. D., *Bioorg. Chem.*, 1981, **10**, 169.
[59] Peterson M. R., Csizmadia I. G., *J. Am. Chem. Soc.*, 1979, **101**, 1076.
[60] Wiberg K. B., Laidig K. E., *J. Am. Chem. Soc.*, 1987, **109**, 5935.
[61] Rebek J. Jr., *Angew. Chem. Int. Ed, Engl.*, 1990, **29**, 245.
[62] Carell C. J., Carell H. L., Erlebacher J., Glusker J. P., *J. Am. Chem. Soc.*, 1988, **110**, 8651.
[63] Marshall L., Parris K., Rebek J. Jr., Luis S. V., Burguete M. I., *J. Am. Chem. Soc.*, 1988, **110**, 5192.
[64] Drew M. G. B., Edwards D. E., Richards R., *J. Chem. Soc. Chem. Commun.*, 1973, 124.
[65] Alcalá R., Fernández García J., *Rev. Acad. Cienc. Exactas Fis.-Quim. Nat. Zaragoza*, 1973, **28**, 303.
[66] Bertaut E. F., Tran Qui D., Burlet P., Thomas M., Moreau J. M. *Acta Cryst.*, 1974, **B30**, 2234.
[67] Lis T., *Acta Cryst.*, 1977, **B33**, 2964.
[68] Puff H., Sievers R., Elsner G., *Z. Anorg. Allg. Chem.*, 1975, **413**, 37.
[69] Clegg W., Little I. R., Straughan B. P., *Acta Cryst.*, 1986, **C42**, 1319.
[70] Post M. L., Trotter J., *J. Chem. Soc. Dalton Trans.*, 1974, 674.
[71] Harrison W., Trotter J., *J. Chem. Soc. Dalton Trans.*, 1972, 956.
[72] Sadikov G. G., Kukina G. A., Porai-Koshits M. A., *J. Struct. Chem.*, 1967, **8**, 492.
[73] Langs D. A., Hare C. R., *J. Chem. Soc. Chem. Commun.*, 1967, 890.
[74] Faggiani R., Brown I. D., *Acta Cryst.*, 1978, **B34**, 2845.
[75] Jelenic I., Grdenic D., Bezjak A., *Acta Cryst.*, 1964, **17**, 758.
[76] Post M. L., Trotter J., *J. Chem. Soc. Dalton Trans.*, 1974, 674.
[77] Freeman H. C., Huq F., Stevens G. N., *J. Chem. Soc. Chem. Commun.*, 1976, 90.
[78] Prout C. K., Carruthers J. R., Rossotti F. J. C., *J. Chem. Soc. A*, 1971, 3350.
[79] Cotton F. A., Diebold M. P., Matusz M., Roth W. J., *Inorg. Chim. Acta*, 1986, **112**, 147.
[80] Catterick J., Hursthouse M. B., New D. B., Thornton P., *J. Chem. Soc. Chem. Commun.*, 1974, 843.
[81] Catterick J., Thornton P., *J. Chem. Soc. Dalton Trans.*, 1976, 1634.
[82] Clegg W., Little I. R., Straughan B. P., *J. Chem. Soc. Chem. Commun.*, 1985, 73.
[83] Clegg W., Little I. R., Straughan B. P., *J. Chem. Soc. Dalton Trans.*, 1986, 1283.
[84] Clegg W., Little I. R., Straughan B. P., *Inorg. Chem.*, 1988, **27**, 1916.
[85] Clegg W., Hunt P. A., Straughan B. P., Antonia Mendiola M., *J. Chem. Soc. Dalton Trans.*, 1989, 1127.
[86] Brown J. N., Trefonas L. M., *Inorg. Chem.*, 1973, **12**, 1730.
[87] Chiari B., Hatfield W. E., Piovesana O., Tarantelli T., ter Haar L. W., Zanazzi P. F., *Inorg. Chem.*, 1983, **22**, 1468.
[88] Rardin R. L., Tolman W. B., Lippard S. J. (unpublished results).
[89] (*a*) Christou G., Perlepes S. P., Folting K., Huffman J. C., Webb R. J., Hendrickson D. N., *J. Chem. Soc. Chem. Commun.*, 1990, 746; (*b*) Christou G., Perlepes S. P., Libby E., Folting K., Huffman J. C., Webb R. J., Hendrickson D. N., *Inorg. Chem.*, 1990, **29**, 3657.
[90] Greenaway A. M., O'Connor C. J., Overman J. W., Sinn E., *Inorg. Chem.*, 1981, **20**, 1508.
[91] Hämäläinen R., Ahlgrén M., Turpeinen U., *Acta Cryst.*, 1982, **B38**, 1577.
[92] Chiari B., Helms J. H., Piovesana O., Tarantelli T., Zanazzi P. F., *Inorg Chem.*, 1986, **25**, 870.
[93] Chiari B., Helms J. H., Piovesana O., Tarantelli T., Zanazzi P. F., *Inorg. Chem.*, 1986, **25**, 2408.
[94] Rardin R. L., Bino A., Lippard S. J., Unpublished results.
[95] Goldberg D., Liu S., Rardin R. L., Lippard S. J., Unpublished results.
[96] Christou G., Personal communication.
[97] Brown S. J., Tao X., Stephan D. W., Mascharak P. K., *Inorg. Chem.*, 1986, **25**, 3377.
[98] Chiari B., Helms J. H., Piovesana O., Tarantelli T., Zanazzi P. F., *Inorg. Chem.*, 1986, **25**, 2408.
[99] Que L. Jr., Personal communication.
[100] Dung N.-H., Viossat B., Busnot A., Sicilia Zafra A. G., Gonzalez Perez J. M., Niclos Gutierrez J., *Inorg. Chim. Acta*, 1990, **169**, 9.
[101] Mak T. C. W., Yip W.-H., O'Reilly E. J., Smith G., Kennard C. H. L., *Inorg. Chim. Acta*, 1985, **100**, 267.
[102] Deacon G. B., Phillips R. J., *Coord. Chem. Rev.*, 1980, **33**, 227.
[103] Luo X.-L., Schulte G. K., Crabtree R. H., *Inorg. Chem.*, 1990, **29**, 682 and references therein.
[104] George G. N., Prince R. C., Cramer S. P., *Science*, 1989, **243**, 789.
[105] Snyder B. S., Patterson G. S., Abrahamson A. J., Holm R. H., *J. Am. Chem. Soc.*, 1989, **111**, 5214 and references therein.
[106] Bürgi H. B., Dunitz J. D., *Acc. Chem. Res.*, 1983, **16**, 153.
[107] Horrocks W. D. Jr., Ishley J. N., Whittle R. R., *Inorg. Chem.*, 1982, **21**, 3270.
[108] Antanaitis B. C., Brown R. D., Chasteen N. D., Fredman J. H., Koenig S. H., Lilienthal H. R., Peisach J., Brewer C. F., *Biochemistry*, 1987, **26**, 7932.
[109] Sorrell T. N., *Tetrahedron*, 1989, **45**, 3.
[110] Stenkamp R. E., Sieker L. C., Jensen L. H., McCallum J. D., Sanders-Loehr J., *Proc. Natl. Acad. Sci.* (*U.S.A.*), 1985, **82**, 713.

[111] Zhang K., Stern E. A., Ellis F., Sanders-Loehr J., Shiemke A. K., *Biochemistry*, 1988, **27**, 7470.
[112] Reem R. C., Solomon E. I., *J. Am. Chem. Soc.*, 1984, **106**, 8323.
[113] Reem R. C., Solomon E. I., *J. Am. Chem. Soc.*, 1987, **109**, 1216.
[114] Maroney M. J., Kurtz D. M. Jr., Nocek J. M., Pearce L. L., Que L. Jr., *J. Am. Chem. Soc.*, 1986, **108**, 6871.
[115] Clark P. E., Webb J., *Biochemistry*, 1981, **20**, 4628.
[116] Lynch J. B., Juarez-Garcia C., Münck E., Que L. Jr., *J. Biol. Chem.*, 1989, **264**, 8091.
[117] Sahlin M., Gräslund A., Petersson L., Ehrenberg A., Sjöberg B.-M., *Biochemistry*, 1989, **28**, 2618.
[118] Fox B. G., Froland W. A., Dege J. E., Lipscomb J. D., *J. Biol. Chem.*, 1989, **264**, 10023.
[119] Fox B. G., Surerus K. K., Münck E., Lipscomb J. D., *J. Biol. Chem.*, 1988, **263**, 10553.
[120] Hathaway B. J., *"Comprehensive Coordination Chemistry"*, Wilkinson G., Gillard R. D., McCleverty J. A. Eds., Pergamon, New York, 1987, Volume 2, p. 413 and references therein.
[121] Keiter R. L., *J. Am. Chem. Soc.*, 1986, **108**, 3846 and references therein.
[122] Shieh M., Martin K. J., Squattrito P. J., Clearfield A., *Inorg. Chem.*, 1990, **29**, 958.
[123] Doi K., Antanaitis B. C., Aisen P., *Struct. Bonding*, 1988, **70**, 1.
[124] Cammack R., Chapman A., Lu W.-P., Karagouni A., Kelly D. P., *F.E.B.S. Lett.*, 1989, **253**, 239.